Journal Name

RSCPublishing

ARTICLE

Cobalt Complexes with Redox-active Anthraquinone-type Ligands

Cite this: DOI: 10.1039/x0xx00000x

Takuya Shiga,* Rina Kumamaru, Graham N. Newton and Hiroki Oshio*

Received 00th January 2012,
Accepted 00th January 2012

DOI: 10.1039/x0xx00000x

www.rsc.org/

Three anthraquinone-type multidentate ligands, $HL^{1\text{-}3}$ (HL = 2-R-1*H*-anthra[1,2-d]imidazole-6,11-dione, HL^1; R = (2-pyridyl), HL^2; R = (4,6-dimethyl-2-pyridyl), HL^3; R = (6-methoxy-2-pyridyl)), were prepared, and their complexation behaviour were investigated. Three bis-chelate cobalt complexes with the formula $[Co^{II}(L^{1\text{-}3})_2]\cdot n(solv.)$ (**1**, **2**, and **3** for HL^1, HL^2, and HL^3, respectively), in which the ligands adopted tridentate binding modes, were synthesized and structurally characterized by single-crystal X-ray analyses. Electrochemical studies of **1**-**3** in CH_2Cl_2 reveal three reversible redox waves, assigned to ligand and cobalt-centred processes. Further complexes were obtained in which HL^1 adopted a bidentate binding mode, stabilising the mono-chelate $[Co^{II}(HL^1)(NO_3)_2(DMF)_2]$ (**4**) species and tris-chelate $[Co^{III}(L^1)_3]$ (**5**) complex in which the cobalt ion was in its 3+ state. The electrochemical properties of complex **5** were investigated in DMF, and the Co(II)/Co(III) redox couple was found to have negatively shifted compared to that of complex **1**, while the ligand-based processes became irreversible. Tridentate chelation is found to stabilise the anthraquinone ligands and unlocks their redox multi-stability.

Introduction

Redox-active ligands, and in particular, non-innocent ligands allow the development of functional coordination compounds with varied and tuneable electronic properties.[1] Indeed, transition metal complexes with redox-active ligands can be successfully employed as reaction sites for a wide range of catalytic molecular conversions.[2] In addition, compounds consisting of redox active metal ions and ligands with similar redox potentials can show significant switchable physical properties arising from intramolecular electron transfer induced by external stimuli (temperature, pressure, light, etc.).[3] From the catalysis perspective, Tanaka *et al.* reported the reduction of carbon dioxide using ruthenium-quinone systems,[4] while Chang *et al.* discovered proton-coupled hydrogen evolution systems based on an *o*-phenylene diamine iron compound.[5] In the development of switchable systems, valence tautomerism was observed in cobalt-dioxolene complexes, and a range of more complicated systems have been reported,[6] some of which were developed by following a rational molecular design approach.[7] Metal dithiolene compounds have been the most studied system due to the strength of the electronic delocalisation between the transition metal centres and the non-innocent ligands.[8] These systems exhibit electrical conductivity based on the formation of a hybrid conduction band comprising ligand p orbitals and metal d orbitals, and have been studied intensively due to their potential applications in molecular electronics.

A substantial body of research in recent years has focussed on advanced materials based on organic donor-acceptor pairs, with systems based on the donor tetrathiafulvalene (TTF) and acceptor tetracyanoquinodimethane (TCNQ) among the most famous and useful for the construction of functional molecular materials.[9] Their analogues have been employed to modify the redox properties of the system and allowed crystal engineering toward functional molecular devices.[10] Electron transfer complexes have attracted attention from the perspective of organic molecular conductors, organic light emission devices and solar batteries, and in order to develop functional molecular compounds, it is important to explore a range of redox-active ligands and to study their complexation behaviour toward metal ions, the potential catalytic applications of such complexes, and the dramatic changes to their electronic states triggered by external stimuli. The molecular design and exploration of redox-active ligands and their complexes underpins this area of research, and such studies will lead to a clear pathway to multifunctional molecular materials.

We previously investigated functional polynuclear complexes based on redox-active ligands incorporating triphenyl amine and ferrocene groups, and their magnetic and electrochemical properties were studied.[11] Dimeric iron complexes with triphenyl amine ligands, $[\{Fe(L)(HL)_2\}\{Fe(HL)_3\}](PF_6)(BF_4)_2\cdot 5CH_3CN\cdot 4H_2O$ and $[\{Fe(L)(HL)_2\}\{Fe(HL)_3\}](PF_6)(FeCl_4)_2$ (HL = 3-(2-pyridyl)-5-[4-(diphenylamino)-phenyl]-1*H*-pyrazole), were found to exhibit SCO and ligand-centered redox behaviour, while a heptanuclear nickel complex with ferrocene groups, $[Ni_7(fcpp)_8(OH)_4](ClO_4)_2\cdot 6CH_3CN$ (Hfcpp = 3-ferrocenyl-5-(2-pyridyl)pyrazole), showed intramolecular antiferromagnetic interactions and ligand-centered redox processes. Both trimethylamine and ferrocene groups can be oxidized to yield stable cationic moieties, and can be used to significantly alter the properties of the molecular assemblies. The combination of multiple redox-active moieties in the same molecular system is a key target towards the generation of functional molecular materials. With this in mind, we focused on the combination of redox-active anthraquinone-type ligands and cobalt ions. The anthraquinone moiety shows two reversible reduction steps at –0.70 and -1.46 V (versus SCE).[12] Examples of coordinative anthraquinone ligands and their complexes have shown that the redox properties of the organic moiety are preserved in the molecular assemblies.[13] In this work, three multidentate anthraquinone-based ligands were synthesised (Scheme 1) and employed to obtain five cobalt complexes. The structural, electronic, electrochemical and luminescent properties of the ligands and their complexes were studied.

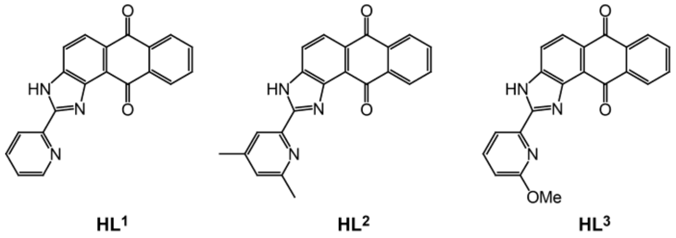

Scheme 1 Anthraquinone-type ligands, HL^1, HL^2, and HL^3

Experimental section

Materials and general methods

All the reagents were commercially purchased and used without further purification.

Syntheses of ligands

The anthraquinone-type ligand HL^1 (Scheme 1) was prepared according to literature,[14] and HL^2 and HL^3 were synthesized by a similar method to that used for HL^1 as described below.

2-(4,6-dimethyl-2-pyridyl)-1H-anthra[1,2-d]imidazole-6,11-dione (HL^2). To a nitrobenzene solution (30 mL) of 1,2-diaminoanthraquinone (725 mg, 3.04 mmol) was added 4,6-dimethyl-2-pyridyl carbaldehyde (402 mg, 2.98 mmol). The resulting brown solution was heated and stirred at 170 °C for 10 h. The reaction mixture was cooled to room temperature, then hexane and ether were added to the solution, affording a brown powder. The brown powder was collected and washed by ether, yielding HL^2 (882 mg, 83.9 %). ^{1}H NMR (400 MHz, $CDCl_3$): δ ppm 2.44 (s, 3H), 2.66 (s, 3H), 7.13 (s, 1H), 7.82-7.84 (m, 2H), 8.12 (s, 1H), 8.15 (d, *J* = 8.4 Hz, 1H), 8.27 (d, *J* = 8.4 Hz, 1H), 8.32-8.38 (m, 2H), 11.98 (s, 1H). Elemental analysis calcd. (%) for $C_{22}H_{15}N_3O_2{\cdot}0.2(H_2O)$: C 74.02, H 4.35, N 11.77; found: C 73.89, H 4.46, N 11.80. IR (KBr): $\tilde{\nu}_{max}$ = 3445, 1665, 1327, 1294, 712 cm^{-1}.

2-(4-methoxy-2-pyridyl)-1H-anthra[1,2-d]imidazole-6,11-dione (HL^3). To a nitrobenzene solution (30 mL) of 1,2-diaminoanthraquinone (714 mg, 3.00 mmol) was added 4-methoxy-2-pyridyl carbaldehyde (0.36 mL, 2.99 mmol). The resulting brown solution was heated at 140 °C for 8 h. After cooling the reaction mixture, hexane and ether were added to the resulting solution, affording yellow powder. The crude products were filtered and washed with ether, yielding HL^3 as a yellow powder (814 mg, 79.9 %) ^{1}H NMR (400 MHz, $CDCl_3$): δ ppm 4.19 (s, 3H), 6.94 (d, *J* = 8.4 Hz, 1H), 7.79 (d, *J* = 7.6 Hz, 1H), 7.81-7.84 (m, 2H), 8.08 (d, *J* = 6.8 Hz, 1H), 8.16 (d, *J* = 8.4 Hz, 1H), 8.27 (d, *J* = 8.4 Hz, 1H), 8.31-8.38 (m, 2H), 11.83 (s, 1H). Elemental analysis calcd. (%) for $C_{21}H_{15}N_3O_3$: C 70.58, H 4.23, N 11.76; found: C 70.56, H 3.93, N 11.84. IR (KBr): $\tilde{\nu}_{max}$ = 3447, 1670, 1574, 1472, 1329, 1298, 714 cm^{-1}.

$[Co^{II}(L^1)_2]{\cdot}H_2O{\cdot}0.5(CH_3OH)$ (1). To a solution of $Co(BF_4)_2{\cdot}6H_2O$ (34.2 mg, 0.1 mmol) in acetonitrile (4 mL) was added HL^1 (32.3 mg, 0.1 mmol) and triethylamine (28 µL, 0.2 mmol) in acetonitrile (8 mL). The colour of the reaction mixture changed to red-brown. After stirring for 5 min, L-ascorbic acid (8.5 mg, 0.05 mmol) in methanol was added. The resulting solution was filtered, and allowed to stand yielding dark brown blocks of $[Co^{II}(L^1)_2]{\cdot}H_2O{\cdot}0.5(CH_3OH)$ (**1**). The crystals were collected by suction and air-dried. Yield 10.41 mg (14 %) Elemental analysis calcd. (%) for $C_{40.5}H_{24}N_6O_{4.5}Co$: C 64.43, H 3.65, N 10.86; found: C 64.26, H 3.76, N 10.96. IR (KBr): $\tilde{\nu}_{max}$ = 1661, 1566, 1327, 1290, 721 cm^{-1}.

$[Co^{II}(L^2)_2]{\cdot}H_2O$ (2). To a solution of $Co(BF_4)_2{\cdot}6H_2O$ (34.0 mg, 0.1 mmol) in acetonitrile (4 mL) was added HL^2 (35.3 mg, 0.1 mmol) and triethylamine (28 µL, 0.2 mmol) in acetonitrile (4 mL) and chloroform (8 mL). After stirring for 5 min, L-ascorbic acid (8.8 mg, 0.05 mmol) in methanol was added. The colour of the reaction mixture changed to dark brown. The resulting solution was filtered and allowed to stand for several days, yielding dark brown plates of $[Co^{II}(L^2)_2]{\cdot}H_2O$ (**2**). The crystals were collected by suction and air-dried. Yield 9.18 mg (12 %). Elemental analysis calcd. (%) for $C_{44}H_{30}N_6O_5Co$: C 67.61, H 3.87, N 10.75; found: C 67.37, H 3.93, N 10.83. IR (KBr): $\tilde{\nu}_{max}$ = 1657, 1560, 1327, 1290, 723 cm^{-1}.

$[Co^{II}(L^3)_2]{\cdot}H_2O{\cdot}0.5(CH_3CN)$ (3). To a solution of $Co(BF_4)_2{\cdot}6H_2O$ (33.5 mg, 0.1 mmol) in acetonitrile (4 mL) was added HL^3 (33.7 mg, 0.1 mmol) and triethylamine (28 µL, 0.2 mmol) in acetonitrile (8 mL). After heating the reaction mixture for 10 minutes, the colour of solution turned to reddish-brown. The resulting solution was filtered, and allowed to stand for several days, yielding dark brown plates of $[Co^{II}(L^3)_2]{\cdot}H_2O{\cdot}0.5(CH_3CN)$ (**3**). The crystals were collected by suction and air-dried. Yield 3.45 mg (4 %). Elemental analysis calcd. (%) for $C_{43}H_{25.5}N_{6.5}O_7Co$: C 64.07, H 3.44, N 11.29; found: C 64.35, H 3.41, N 11.40. IR (KBr): $\tilde{\nu}_{max}$ = 1663, 1568, 1477, 1327, 1294, 1283, 718 cm^{-1}.

$[Co^{II}(HL^1)(NO_3)_2(DMF)_2]{\cdot}H_2O$ (4). To a solution of $Co(NO_3)_2{\cdot}6H_2O$ (29.2 mg, 0.1 mmol) in DMF (2 mL) was added HL^1 (32.7 mg, 0.1 mmol). The colour of the reaction mixture changed to dark brown, then stirred for 10 minutes at room temperature. The resulting solution was filtered, and diffused with *o*-xylene yielding thin dark brown plates of $[Co^{II}(HL^1)(NO_3)_2(DMF)_2]{\cdot}H_2O$ (**4**). The crystals were collected by suction and air-dried. Yield 23.9 mg (36 %). Elemental analysis calcd. (%) for $C_{26}H_{27}N_7O_{11}Co$: C 46.44, H 4.05, N 14.58; found: C 46.75, H 4.14, N 14.68. IR (KBr): $\tilde{\nu}_{max}$ = 1668, 1649, 1443, 1385 (NO_3), 1329, 1308, 719 cm^{-1}.

$[Co^{III}(L^1)_3]{\cdot}4(H_2O){\cdot}CH_3CN$ (5). The filtrate of the reaction solution in the synthesis of **1** was left to stand for several days, yielding red crystals of $[Co^{III}(L^1)_3]{\cdot}4(H_2O){\cdot}CH_3CN$ (**5**). Yield 0.68 mg (0.02 %). The crystals were collected by suction and air-dried. Elemental analysis calcd. (%) for $C_{62}H_{41}N_{10}O_{10}Co$: C 65.04, H 3.61, N 12.23; found: C 65.34, H 3.54, N 12.09. IR (KBr): $\tilde{\nu}_{max}$ = 1667, 1445, 1327, 1287, 851, 718 cm^{-1}.

$[Zn^{II}(L^1)_2]$ (6). To a solution of $Zn(BF_4)_2{\cdot}nH_2O$ (23.8 mg, 0.1 mmol) in acetonitrile (2 mL) was added HL^1 (32.5 mg, 0.1 mmol) and triethylamine (28 µL, 0.2 mmol) in acetonitrile (4 mL). The reaction mixture was stirred for 5 minutes. The resulting solution was filtered, and allowed to stand for several days, yielding thin dark brown plates of $[Zn^{II}(L^1)_2]$ (**6**). Yield 1.20 mg (2 %). The crystals were collected by suction and air-dried. Elemental analysis calcd. (%) for $C_{40}H_{20}N_6O_4Zn$: C 67.29, H 2.82, N 11.77; found: C 67.29, H 3.17, N 11.81. IR (KBr): $\tilde{\nu}_{max}$ = 1659, 1568, 1441, 1325, 1292, 718 cm^{-1}.

X-ray crystallography

Data collections were performed on a Bruker SMART APEX II for all complexes, with a CCD area detector with graphite monochromated Mo-K_α (λ = 0.71073 Å) radiation. All structures were solved by direct methods and refined by full-matrix least-squares methods based on F^2 using the SHELXL software.[15] Non-hydrogen atoms were refined anisotropically. All hydrogen atoms were positioned geometrically and refined with isotropic displacement parameters according to the riding model. All geometrical calculations were performed using the SHELXL software.

Physical measurements

Infrared (IR) spectra were recorded (400-4000 cm^{-1} region) on a SHIMADZU FT-IR 8400 spectrometer using KBr pellets. Cyclic voltammetry measurements were carried out in a standard one-compartment cell under N_2 at 20 °C equipped with a platinum-wire counter electrode, an SCE reference electrode, and a glassy carbon (GC) working electrode using a BAS 620A electrochemical analyser. The measurements were performed in CH_2Cl_2 or DMF (for complex **5**) with 0.1 M tetra-n-butylammonium hexafluorophosphate (n-Bu_4NPF_6) as the supporting electrolyte. Analyte concentrations for all ligands and complexes were 0.6 mM. In the measurement of HL^1 in DMF, a concentration of 1.0 mM was used. The E values were references to the $E_{1/2}$ value of ferrocene, which was measured under identical conditions each time. UV-vis absorption spectra were recorded on SHIMADZU UV-3150 spectrometer. Fluorescence spectra were measured by JASCO FP-8500 spectrofluorometer at room temperature. Absolute quantum yields were determined using an integrating sphere photometer. Measurements were performed using degassed solvent.

Results and discussion

Syntheses

The anthraquinone-type ligand HL^1 (Fig. 1, R = (2-pyridyl)) was originally reported in reference 11, in which Ru and Ir complexes were studied. In this paper, two analogous ligands HL^2 (R = (4,6-dimethyl-2-pyridyl)) and HL^3 (R = (6-methoxy-2-pyridyl)) were synthesized according to the literature.[16] Three bis-chelate cobalt complexes, $[Co^{II}(L^{1\text{-}3})_2]\cdot n(\text{solv.})$ (**1**, **2**, and **3** for HL^1, HL^2, and HL^3, respectively) were synthesized using similar synthetic methods. L-ascorbic acid was added as an antioxidant, and was found to improve product purity, particularly in the synthesis of **3**. When using HL^1, the mono-dentate $[Co^{II}(HL^1)(NO_3)_2(DMF)_2]$ (**4**) and tris-chelate cobalt complexes $[Co^{III}(L^1)_3]$ (**5**) were obtained by slight modification of the synthetic method. The ligands have two coordination modes, the bidentate N_2 mode of pyridine benzimidazole chelate, and the tridentate N_2O mode in which the additional quinone oxygen is also binding. The benzimidazole moiety of the ligands has a dissociative proton, thus the ligands can be neutral or mono-anionic. This flexibility allows the ligands to stabilise complexes in a range of different ways.

In order to elucidate the electrochemical character of HL^1, a zinc complex, $[Zn^{II}(L^1)_2]$ (**6**), was synthesized as a reference. Complexes **1**, **4** and **5** were bis-, mono-, and tris-chelate complexes with the same ligand HL^1, respectively. Selective syntheses of these complexes were achieved by optimization of the reagent ratio and selection of solvent. The mono-chelate complex **4** was synthesized without base in DMF solution, which is a coordinative solvent. Complexes **1** and **5** can be obtained by the same synthetic method, but can be separated by their different solubilities.

Molecular structures

The molecular structures of complexes **1-6** were determined by single-crystal X-ray diffraction analysis. Complexes **1-3**, which have a bis-chelate mode, have similar structures. As an example, the structural features of complex **1** are described here in detail. **1** crystalized in triclinic space group $P\overline{1}$ and consists of two HL^1 ligands, one cobalt ion and solvent molecules in the lattice. The ligands coordinate the cobalt ion in the tridentate *mer* manner. The cobalt ion has an octahedral coordination geometry of N_4O_2 donor atoms, of which two are pyridine and two are imidazole nitrogen atoms and the two oxygen atoms are donated by the anthraquinone moiety. The average coordination bond length is 2.163(10) Å. Therefore, the cobalt ion is divalent based on BVS calculations[17] and charge balance. The imidazole moiety of the ligand is deprotonated and the ligands are mono-anionic. The bond length of C=O is 1.226(3)-1.227(3) Å, indicating that the group is in the keto form. The structural distortion parameter, Σ (the sum of the deviation of each of the 12 *cis* N/O-Co-N/O angles from 90°), is 128.83°. Complexes **2** and **3** have similar bis-chelate coordination of the Co(II) ion, but there are slight differences in the structure around the metal ions owing to steric hindrance of the substituent groups. In **2** and **3**, with methyl group and methoxy moiety, the average coordination bond lengths are 2.196(6) and 2.160(3), respectively. Σ values for **2** and **3** are 109.77° and 107.80°, respectively. In **1-3**, it is considered that the ligands are deprotonated based on charge balance. X-ray structural analysis was also performed for the control complex **6**. The molecular structure of **6** is almost identical to complex **1**.

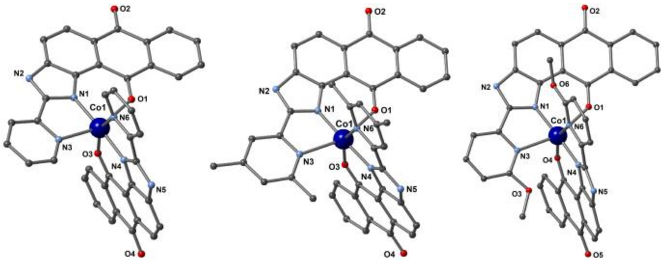

Figure 1 Molecular structure of **1** (left), **2** (centre), and **3** (right). All H atoms have been omitted for clarity. Color code: Co, blue; N, light-blue; O, red; C, gray.

Single crystal X-ray analysis reveals that **4** consists of one ligand HL^1, one cobalt ion, two nitrate ions and one DMF molecule. The ligand coordinates the cobalt ion in a bidentate fashion. The cobalt ion has octahedral coordinate geometry with two nitrogen atoms from HL^1 and four oxygen donor atoms from the nitrate and DMF groups. Considering the coordination bond lengths, BVS calculations[14], and charge balance, the cobalt ion in **4** can be assumed to be divalent and the ligand HL^1 protonated.

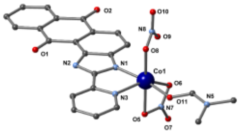

Figure 2 Molecular structure of **4**. All H atoms have been omitted for clarity. Color code: Co, blue; N, light-blue; O, red; C, gray.

Table 1. Crystallographic data.

Complex	**1**	**2**	**3**	**4**	**5**	**6**
Formula	$C_{42}H_{26}N_6O_6Co$	$C_{44}H_{28}N_6O_4Co$	$C_{44}H_{27}N_7O_6Co$	$C_{55}H_{57}N_{15}O_{21}Co_2$	$C_{70.25}H_{45}N_{13}O_{8.25}Co$	$C_{40}H_{20}N_6O_4Zn$
Formula Weight	769.62	763.65	808.66	1382.01	1262.12	713.99
Temperature (K)	100(2)	100(2)	100(2)	100(2)	100(2)	100(2)
Wavelength (Å)	0.71073	0.71073	0.71073	0.71073	0.71073	0.71073
Crystal system	Monoclinic	Triclinic	Triclinic	Monoclinic	Triclinic	Triclinic
Space group	$P2_1/c$	$P\bar{1}$	$P\bar{1}$	$P2_1$	$P\bar{1}$	$P\bar{1}$
a (Å)	12.1799(18)	10.334(4)	10.0343(17)	13.525(6)	12.720(3)	10.681(3)
b (Å)	17.818(3)	11.306(4)	11.1530(18)	13.060(6)	15.676(3)	10.758(2)
c (Å)	16.549(2)	14.456(6)	17.350(3)	17.173(8)	16.500(3)	14.402(3)
α (°)	-	97.909(7)	97.659(3)	-	73.155(3)	94.847(4)
β (°)	107.1566(19)	91.932(6)	93.997(3)	102.295(7)	74.382(3)	93.595(4)
γ (°)	-	92.549(6)	110.028(3)	-	76.188(3)	114.278(4)
Volume (Å^3)	3431.6(9)	1669.9(11)	1794.0(5)	2964(2)	2986.2(10)	1494.5(6)
Z	4	2	2	2	2	2
Density (calc.) (Mg m^{-3})	1.490	1.519	1.497	1.549	1.404	1.587
Absorption coeff. (mm^{-1})	0.562	0.573	0.542	0.652	0.360	0.881
Crystal size (mm^3)	0.25×0.20×0.10	0.20×0.10×0.05	0.20×0.20×0.05	0.30×0.25×0.05	0.30×0.30×0.30	0.40×0.20×0.20
Reflections collected	18971	9679	9586	16483	16025	8171
Independent reflections	7813 [R(int) = 0.0311]	7347 [R(int) = 0.0989]	6522 [R(int) = 0.0313]	9468 [R(int) = 0.0810]	10882 [R(int) = 0.0258]	5454 [R(int) = 0.0213]
Data/restraints/parameters	7813/498/0	7347/500/0	6522/526/0	9468/848/207	10882/870/6	5454/460/0
Goodness-of-fit on F^2	1.163	1.092	1.030	1.294	1.085	0.849
Final R indices [$I > 2\sigma(I)$]	$R_1 = 0.0489$ $wR_2 = 0.1426$	$R_1 = 0.0887$ $wR_2 = 0.1894$	$R_1 = 0.0723$ $wR_2 = 0.1647$	$R_1 = 0.1034$ $wR_2 = 0.2405$	$R_1 = 0.0627$ $wR_2 = 0.1638$	$R_1 = 0.0441$ $wR_2 = 0.1135$
R indices (all data)	$R_1 = 0.0721$ $wR_2 = 0.1656$	$R_1 = 0.2426$ $wR_2 = 0.2648$	$R_1 = 0.0939$ $wR_2 = 0.1786$	$R_1 = 0.1530$ $wR_2 = 0.2663$	$R_1 = 0.0800$ $wR_2 = 0.1754$	$R_1 = 0.0547$ $wR_2 = 0.1203$
Largest diff. peak and hole (e Å^{-3})	0.850 and -0.478	0.620 and -0.675	0.637 and -0.392	2.074 and -1.058	1.088 and -0.862	0.901 and -0.751
CCDC number	1823330	1823331	1823332	1823333	1823334	1823335

Complex **5** is a tris-chelate system, in which the bidentate site of the ligand coordinates the cobalt ion, and the ligands are deprotonated and monoanionic. The C=O bond length of the ligand is slightly short (1.216(4) - 1.222(4) Å), compared to that of protonated ligand. There are no counter anions, and BVS calculations confirm that the cobalt ion is in its trivalent state.[14] The average coordination bond lengths, 1.938(3) Å, are shorter than those of complexes **1-4**. Each ligand has two kinds of nitrogen donor atoms; pyridyl and imidazolyl. The ligands are orientated around the cobalt ion such that the three pyridine donors coordinate to cobalt ions in the *mer* mode, as do the benzimidazole moieties.

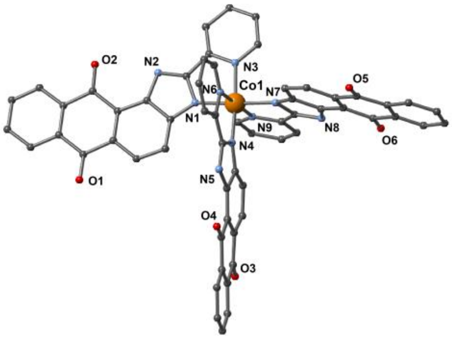

Figure 3 Molecular structure of **5**. All H atoms have been omitted for clarity. Color code: Co, Orange; N, light-blue; O, red; C, gray.

Electrochemical properties

Electrochemical properties of the three ligands and complexes **1-3**, **5** and **6** were investigated. The data collected for **6** was used as a control sample. Cyclic voltammetry of the ligands and complexes was performed in CH_2Cl_2 solution and recorded relative to a SCE reference electrode. The resultant voltammograms are shown in Fig. 4, and the redox potentials ($E_{1/2}$) and assignments are provided in Table 1.

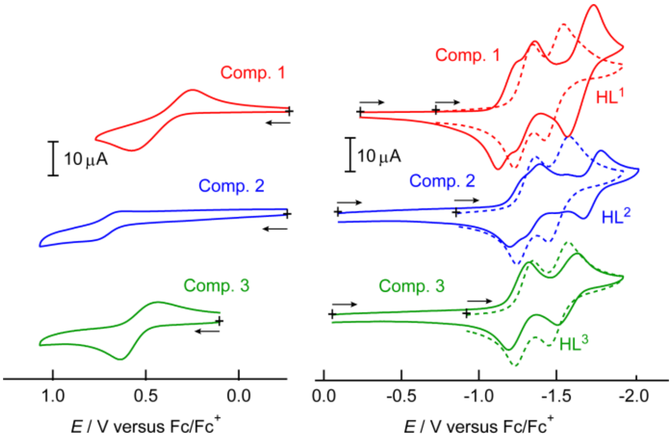

Figure 4 Cyclic voltammograms of ligand HL$^{1-3}$ (dotted lines, red, blue and green for HL^1, HL^2 and HL^3, respectively), and **1-3** (solid lines, red, blue and green for **1**, **2** and **3**, respectively). Open circuit potentials are indicated by the black crosses, and scan directions by the arrows.

Table 2. Selected coordination bong lengths (Å).

Complex **1**		Complex **2**		Complex **3**		Complex **4**			
Co-N1	1.967(2)	Co-N1	1.967(6)	Co-N1	1.965(3)	Co1-N1	2.078(10)	Co2-N4	2.099(9)
Co-N3	2.227(2)	Co-N3	2.311(6)	Co-N3	2.268(3)	Co1-N3	2.156(8)	Co2-N6	2.184(7)
Co-N4	1.979(2)	Co-N4	1.974(5)	Co-N4	1.958(3)	Co1-O5	2.201(9)	Co2-O12	2.151(9)
Co-N6	2.213(2)	Co-N6	2.287(6)	Co-N6	2.264(3)	Co1-O6	2.194(8)	Co2-O15	2.083(8)
Co-O1	2.3597(18)	Co-O1	2.269(6)	Co-O1	2.304(3)	Co1-O8	2.173(14)	Co2-O18	2.063(9)
Co-O3	2.2296(17)	Co-O3	2.370(5)	Co-O4	2.198(3)	Co1-O11	2.047(10)	Co2-O19	2.075(7)

Complex **5**		Complex **6**	
Co-N1	1.925(2)	Zn-N1	1.961(2)
Co-N3	1.958(3)	Zn-N3	2.115(2)
Co-N4	1.919(3)	Zn-N4	1.947(2)
Co-N6	1.951(2)	Zn-N6	2.195(2)
Co-N7	1.926(2)	Zn-O1	2.724(2)
Co-N9	1.947(3)	Zn-O3	2.524(2)

According to the literature, anthraquinone shows two reversible reduction process at -1.13 and -1.89 V versus Fc/Fc^+ in NMP, which are attributed to Quinone (Q) / Semiquinone ($SQ^{\bullet -}$) and Semiquinone ($SQ^{\bullet -}$) / Catecolate (Cat^{2-}) redox waves, respectively. [18] HL^1 shows two reduction waves at -1.29 and -1.49 V. The first reduction process is slightly more positive than that of anthraquinone due to the substituent effect of the benzimidazole moieties. HL^2 and HL^3 show similar two-step reduction processes. Differences between the redox properties of the different ligands are negligible, indicating that the influence of the pyridine substituents on the quinone moiety is weak.

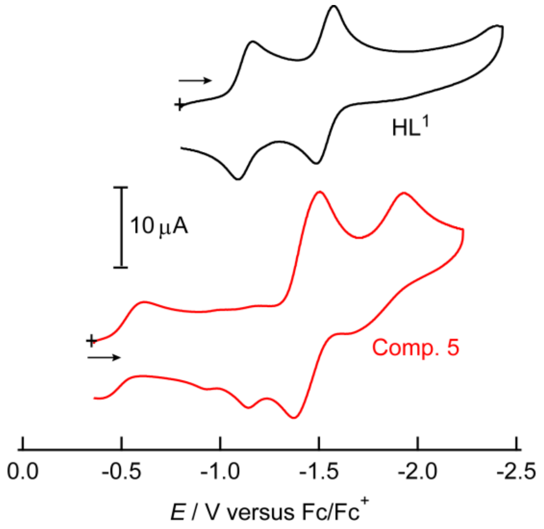

Figure 5 Cyclic voltammograms of ligand HL^1 and **5**. Open circuit potentials are indicated by the black crosses, and scan directions by the arrows.

Complexes **1**, **2**, and **3** show three quasi-reversible redox waves, two of which can be assigned to ligand-based processes, and the other to the reversible oxidation of the cobalt centre. The redox processes around -1.18 ~ -1.36 V can be assigned as Quinone (Q) / Semiquinone ($SQ^{\bullet -}$), while the waves at -1.66 ~ -1.57 V can be considered as Semiquinone ($SQ^{\bullet -}$) / Catecholate (Cat) processes. The redox wave of the ligand-based $Q/SQ^{\bullet -}$ process in the voltammograms of **1** and **2** is slightly split due to intra-molecular electronic communication between the two ligands through the cobalt centre, suggesting that the molecule is electronically conjugated through the metal ion. The $SQ^{\bullet -}/Cat^{2-}$ processes were negatively shifted compared with the free ligands. The reason for this negative shift is likely due to the dianonc charge of the two-electron reduced complexes.

Table 3. Redox potentials (versus Fc/Fc^+).

Compounds	Assignments		
	Co(II)/Co(III)	$Q/SQ^{\bullet -}$	$SQ^{\bullet -}/Cat^{2-}$
HL^1		-1.29	-1.49
HL^2		-1.31	-1.52
HL^3		-1.29	-1.51
Comp.1	0.38	-1.18, -1.31	-1.66
Comp.2	0.70	-1.24, -1.36	-1.73
Comp.3	0.54	-1.26	-1.57
Comp.6		-1.02, -1.16	-1.73
HL^1 [a]		-1.14	-1.52
Comp.5 [a]	-0.49	-1.14 ~ -1.50	-1.82

[a] measured in DMF

The oxidation potentials of the cobalt ion appeared in the range of 0.38 – 0.70 V, with the oxidation peak of **1** falling at more negative potential than that of **2** and **3**. Considering the electron donation effects of the substituent groups, which would typically result in a negative potential shift in the redox chemistry of a coordinated metal centre due to the increased ligand basicity, the tendency of the potential shift is the opposite of that expected. The positive shifts observed in the cobalt redox in compounds **2** and **3** can be explained by examining the structural features of the complexes. Note that coordination bond lengths about cobalt(II) ions tend to be shorted as the oxidation to cobalt(III) ions. There is substantial steric hindrance introduced by the substituent groups in **2** and **3**, and this will disfavour the required structural changes, resulting in a positive shift in the oxidation potential of the cobalt ion. In the case of complex **5**, irreversible redox waves were observed in the potential range of -1.02 ~ -1.73 V, which are assigned to $Q/SQ^{\bullet -}$ and $SQ^{\bullet -}/Cat^{2-}$ processes, accompanied with protonation or decomposition. A Co(II)/Co(III) redox process was observed at -0.06 V, which is close to the redox potentials of previously reported cobalt complexes with tris azole heterocycle ligands. [19] Cyclic voltammetry of complex **6**, the zinc derivative with HL^1, was measured for comparison (Supporting info, Figure S1). There were three reduction waves attributed to ligand reduction processes, at similar potentials to those of complex **1**.

Luminescent properties

9,10-anthraquinone shows luminescence at 412 nm, and HL^1 shows emission at 562 nm.[16] The three ligands, HL^1, HL^2 and HL^3, show similar absorption and broad fluorescence to the reported one (Figure 6a). Broad transitions around 350-450 nm for the ligands (395, 398 and 405 nm for HL^1, HL^2 and HL^3, respectively) can be assigned as ILCT (= intra-ligand charge transfer) transitions, while the emission bands at 519, 523 and 540 nm for HL^1, HL^2 and HL^3, respectively, are derived from ILCT excited states.[17] The absolute quantum yields of HL^1, HL^2 and HL^3 were determined to be 0.95, 1.75 and 4.24 %, respectively. The similarity of the general spectroscopic features of the three ligand derivatives indicates that substituent groups on the pyridine ring exert minimal influence on the electronic properties of the anthraquinone moiety.

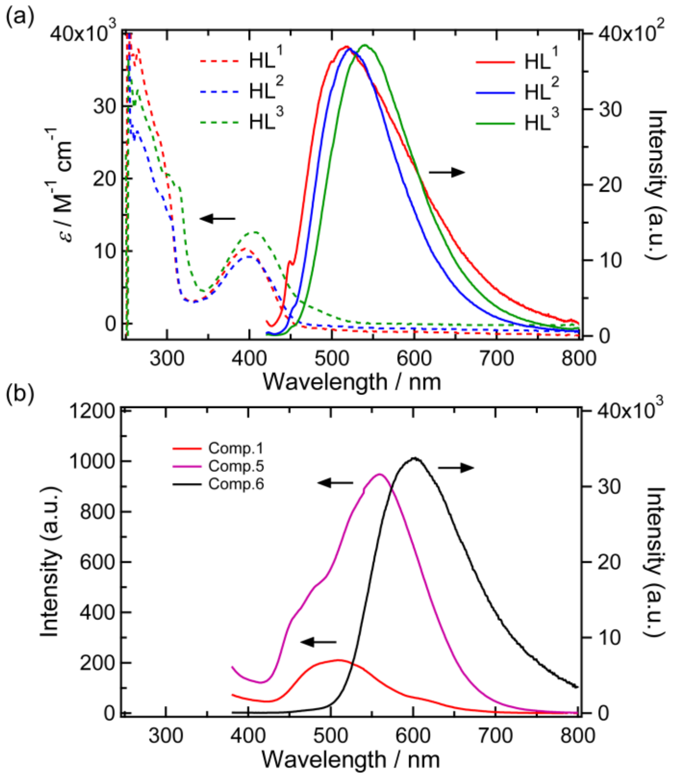

Figure 6 (a) UV-vis spectra and emission spectra of ligands HL^{1-3} In DMF solution (0.01mM). (b) Luminescent properties of **1**, **5** and **6**.

The luminescence properties of complexes **1**, **5** and **6** were investigated and these spectra are shown in Figure 6b. Complex **1** shows relatively weak emission around 500 nm, while complexes **5** and **6** show stronger emission around 550-600 nm. The reason for the weak emission of **1** can be understood as paramagnetic quenching due to the Co(II) centre and effect of dissociation equilibrium of the complex. The bathochromic shifts of the emission bands of **5** and **6** were caused by the decrease in LUMO energy effected by the charge and acidity of the coordinated metal ion. Luminescence spectra for **1-3** are shown in Figure S2, and exhibit small differences depending on the spectroscopic properties of HL^1-HL^3 respectively. These tuneable luminescent properties and solution stability may lead to potential applications in future switchable photochemical systems.

Conclusion

In this work, new cobalt complexes with redox-active anthraquinone-type multidentate ligands were synthesized, and their electrochemical and luminescent properties were investigated. Three anthraquinone-type multidentate ligands, HL^{1-3} (HL = 2-R-1*H*-anthra[1,2-d]imidazole-6,11-dione, HL^1; R = (2-pyridyl), HL^2; R = (4,6-dimethyl-2-pyridyl), HL^3; R = (6-methoxy-2-pyridyl)), were prepared from carboxylates and diamines. Complexation studies with the ligands yielded three bis-chelate cobalt complexes $[Co^{II}(L^{1-3})_2]\cdot n(solv.)$ (**1**, **2**, and **3** for HL^1, HL^2, and HL^3, respectively), which were structurally characterized by single-crystal X-ray analyses. Electrochemical studies performed on **1-3** reveal three reversible redox waves assigned to ligand reduction and Co(II)/Co(III) oxidation processes. In addition, mono-chelate $[Co^{II}(HL^1)(NO_3)_2(DMF)_2]$ (**4**) and tris-chelate complexes $[Co^{III}(L^1)_3]$ (**5**) were synthesized, revealing the anthraquinone ligands to act as bidentate or tridentate chelates depending on the complexation conditions. These compounds demonstrate the varied approach to the construction of multi-redox coordination complexes and may aid in the design and synthesis of the next generation of non-innocent ligand supported transition metal molecular catalysts.

Acknowledgements

This work was supported by a JSPS KAKENHI Grant Number JP16H06523 (Coordination Asymmetry). This work was also supported by a Grant-in-Aid for Scientific Research (C) (Grant No. 17K05800) and Tokuyama Science Foundation. The authors thank Dr. Masayuki Miura (JASCO corp.) for absolute quantum yield measurements.

Notes and references

[a] Graduate School of Pure and Applied Sciences, University of Tsukuba, Tennodai 1-1-1, Tsukuba 305-8571, Japan. E-mail: shiga@chem.tsukuba.ac.jp, oshio@chem.tsukuba.ac.jp

[b] GSK Carbon Neutral Laboratories for Sustainable Chemistry, University of Nottingham, Jubilee Campus, Nottingham, NG7 2GA, UK.

Electronic Supplementary Information (ESI) available: Electrochemical properties of **6**, and luminescence properties for **1-3**. CCDC 1823330-1823335 for **1** - **6**, respectively. For ESI and crystallographic data in CIF or other electronic format see DOI: 10.1039/b000000x/

1 W. Kaim and B. Schwederski, *Coord. Chem. Rev.*, 2010, **254**, 1580-1588; W. Kaim, *Coord. Chem. Rev.*, 1987, **76**, 187-235; V. Lyaskovskyy and B. des Bruin, *ACS Catal.*, 2012, **2**, 270-279.

2 O.R. Luca and R.H. Crabtree, *Chem. Soc. Rev.*, 2013, **42**, 1440-1459; *ACS Catal.*, 2012, **2**, 270-279.

3 C.G. Pierpont, *Coord. Chem. Rev.*, 2001, **219-221**, 415-433; C.G. Pierpont, *Coord. Chem. Rev.*, 2001, **216-217**, 99-125; A.I. Poddel'sky, V.K. Cherkasov and G.A. Abakumov, *Coord. Chem. Rev.*, 2009, **253**, 291-324; A. Mederos, S. Domínguez, R. Hernández-Molina, J. Sanchiz and Felipe Brito, *Coord. Chem. Rev.*, 1999, **193-195**, 857-911.

4 K. Tanaka and D. Ooyama, *Coord. Chem. Rev.*, 2002, **226**, 211-218; K. Tanaka, *Chem. Rec.*, 2009, **9**, 169-186; H. Ohtsu and K. Tanaka, *Chem. Commun.*, 2012, **48**, 1796-1798; T. Fukushima, D. Ghosh, K. Kobayashi, H. Ohtsu, S. Kitagawa and K. Tanaka, *Inorg. Chem.*, 2016, **55**, 11613-11616.

5 T. Matsumoto, H.-C. Chang, M. Wakizaka, S. Ueno, A. Kobayashi, A. Nakayama, T. Taketsugu and M. Kato, *J. Am. Chem. Soc.*, 2013, **135**, 8646-8654.

6 K.G. Alley, G. Poneti, P.S.D. Robinson, A. Nafady, B. Moubaraki, J.B. Aitken, S. C. Drew, C. Ritchie, B. F. Abrahams, R. K. Hocking, K. S. Murray, A. M. Bond, H. H. Harris, L. Sorace and C. Boskovic, *J. Am. Chem. Soc.*, 2013, **135**, 8304-8323; K.G. Alley, G. Poneti, J.B. Aitken, R.K. Hocking, B. Moubaraki, B.F. Abrahams, H.H. Harris, L. Sorace and C. Boskovic, *Inorg. Chem.*, 2012, **51**, 3944-3946; O. Drath, R. W. Gable, B. Moubaraki, K.S. Murray, G. Poneti, L. Sorace and C. Boskovic, *Inorg. Chem.*, 2015, **55**, 4141-4151; J. Dai, S. Kanegawa, Z. Li, S. Kang and O. Sato, *Eur. J. Inorg. Chem.*, 2013, 4150-4153; J. Tao, H. Maruyama and O. Sato, *J. Am. Chem. Soc.*, 2006, **128**, 1790-1791; S. K. Larsen and C. G. Pierpont, *J. Am. Chem. Soc.*, 1988, **110**, 1827-1832; M.A. Ribeiro, M. Lanznaster, M.M. P. Silva, J.A.L.C. Resende, M.V.B. Pinheiro, K. Krambrock, H.O. Stumpf and C. B. Pinheiro, *Dalton Trans.*, 2013, **42**, 5462-5470.

7 O. Sato, A. Cui, R. Matsuda, J. Tao and S. Hayami, *Acc. Chem. Res.*, 2007, **40**, 361-369; T. Tezgerevska, K. G. Alley and C. Boskovic, *Coord. Chem. Rev.*, 2004, **268**, 23-40.

8 R. Kato, *Chem. Rev.*, 2004, **104**, 5319-5346; H.-B. Duan, X.-M. Ren and Q.-J. Meng, *Coord. Chem. Rev.*, 2010, **254**, 1500-1522; B. Garreau-de Bonneval, K.I. M.-C. Ching, F. Alary, T.-T. Bui and L. Valade, *Coord. Chem. Rev.*, 2010, **254**, 1457-1467; P. Deplano, L. Pilia, D. Espa, M. L. Mercuri, A. Serpe, *Coord. Chem. Rev.*, 2010, **254**, 1434-1447.

9 J. Ferraris, D.O. Cowan, V. Walatka and J. H. Perlstein, *J. Am. Chem. Soc.*, 1973, **95**, 948-949; D. Jérome, *Chem. Rev.*, 2004, **104**, 5565-5591.

10 A. Das and S. Ghosh, *Angew. Chem. Int. Ed.*, 2014, **53**, 2038-2054; G. Saito, Y. Yoshida, *Bull. Chem. Soc. Jpn.*, 2007, **80**, 1-137; S. Horiuchi, F. Ishii, R. Kumai, Y. Okimoto, H. Tachibana, N. Nagaosa, Y. Tokura, *Nat. Mat.*, 2005, **4**, 163-166.

11 G.N. Newton, K. Mitsumoto, R.-J. Wei, F. Iijima, T. Shiga, H. Nishikawa, H. Oshio, *Angew. Chem. Int. Ed.*, 2014, **53**, 2941-2944; K. Mitsumoto, M. Nihei, T. Shiga, H. Oshio, *Chem. Lett.*, 2008, **37**, 966-967; T. Shiga, E. Oshiro, N. Nakayama, K. Mitsumoto, G.N. Newton, H. Nishikawa, H. Oshio, *Eur. J. Inorg. Chem.*, 2013, 781-787.

12 P. Zuman, Collect. Czech. *Chem. Commun.*, 1962, **27**, 2035; J. Q. Chambers, Electrochemistry of quinones, in The Chemistry of the Quinonoid Compounds, ed. S. Patai and Z. Rappoport, Wiley, Toronto, 1988, p. 719.

13 T. Ruffer, B. Brauere, F.E. Meva, B. Walfort, *Dalton Trans.*, 2008, 5089-5098; C.J. da Cunha, S.S. Fielder, D.V. Stynes, H. Masui, P.R. Auburn, A.B.P. Lever, *Inorg. Chim. Acta*, 1996, **242**, 293-302.

14 X. Peng, Y. Wu, J. Fan, M. Tian and K. Han, *J. Org. Chem.*, 2005, **70**, 10524-10531; A.J. Hallet, B.D. Ward, B.M. Kariuki, S.J.A. Pope, *J. Organomet. Chem.*, 2010, **695**, 2401-2409; Y.-X. Yuan, Y. Chen, Y.-C. Wang, C.-Y. Su, S.-M. Liang, H. Chao and L.-N. Ji, *Inorg. Chem. Commun.*, 2008, **11**, 1048-1050; V. Luxami and S. Kumar, *Dalton Trans.*, 2012, **41**, 4588-4593; T. T. Guimarães, E. N. Da Silva Júnior, C. E. M. Carvalho, C. A. De Simone and A. V. Pinto, *Acta Cryst.*, 2009, **E65**, o1063; A. Sarkar, S. Bhattacharyya and A. Mukherjee, *Dalton Trans.*, 2016, **45**, 1166-1175.

15 G.M. Sheldrick, *SHELXL-2013*; University of Göttingen: Göttingen, Germany, 2013; G.M. Sheldrick, SHELXTL-PC Package; Bruker AXS, Inc.

16 S.A. Carlson and D.M. Hercules, *Anal. Chem.*, 1973, **45**, 1794-1799; S.A. Carlson and D.M. Hercules, *Photochem. Photobiol.*, 1973, **17**, 123-131; A.J. Hallett, B.D. Ward, B.M. Kariuki, S.J.A. Pope, *J. Organomet. Chem.*, 2010, **695**, 2401-2403; P. Dahiya, M. Kumbhakar, D.K. Maity, T. Mukherjee, J.P. Mittal, A.B.R. Tripathi, N. Chattopadhyay and H. Pal, *Photochem. Photobiol. Sci.*, 2005, **4**, 100-105.

17 BVS calculation for **1**, 1.663 for Co(II), 2.000 for Co(III); for **2**, 1.558 for Co(II), 1.875 for Co(III); for **3**, 1.686 for Co(II), 2.010 for Co(III); for Co1 in **4**, 1.610 for Co(II), 2.110 for Co(III); for Co2 in **4**, 1.746 for Co(II), 2.288 for Co(III); for **5**, 2.760 for Co(II), 3.616 for Co(III).

18 J.E. Gautrot, P. Hodge, D. Cupertino, M. Helliwell, *New J. Chem.*, 2006, **30**, 1801-1807.

19 N.M. Shavaleev, F. Kessler, M. Gratzel, M.K. Nazeeruddin, *Inorg. Chim. Acta*, 2013, **407**, 261-268.